Journal of Neurochemistry JNC

JOURNAL OF NEUROCHEMISTRY | 2012 doi: 10.1111/j.1471-4159.2012.07707.x

ORIGINAL ARTICLE

N-Terminal pyroglutamate formation of Aβ38 and Aβ40 enforces oligomer formation and potency to disrupt hippocampal long-term potentiation

Dagmar Schlenzig,* Raik Rönicke,† Holger Cynis,* Hans-Henning Ludwig,* Eike Scheel,* Klaus Reymann,† Takaomi Saido,‡ Gerd Hause,§ Stephan Schilling* and Hans-Ulrich Demuth*

*Probiodrug AG, Halle/Saale, Germany

†Deutsches Zentrum für Neurodegenerative Erkrankungen, c/o Leibniz-Institut für Neurobiologie, Magdeburg, Germany

‡Laboratory of Proteolytic Neuroscience, RIKEN Brain Science Institute, Wako, Saitama, Japan

§Biozentrum der Martin-Luther-Universität, Halle/Saale, Germany

Abstract

Pyroglutamate (pGlu)-modified amyloid peptides have been identified in sporadic and familial forms of Alzheimer's disease (AD) and the inherited disorders familial British and Danish Dementia (FBD and FDD). In this study, we characterized the aggregation of amyloid-β protein Aβ37, Aβ38, Aβ40, Aβ42 and ADan species *in vitro*, which were modified by N-terminal pGlu (pGlu-Aβ3-x, pGlu-ADan) or possess the intact N-terminus (Aβ1-x, ADan). The pGlu-modification confers rapid formation of oligomers and short fibrillar aggregates. In accordance with these observations, the pGlu-modified Aβ38, Aβ40 and Aβ42 species inhibit hippocampal long term potentiation of synaptic response, but pGlu-Aβ3-42 showing the highest effect. Among the unmodified Aβ peptides, only Aβ1-42 exhibites such propensity, which was similar to pGlu-Aβ3-38 and pGlu-Aβ3-40. Likewise, the amyloidogenic peptide pGlu-ADan impaired synaptic potentiation more pronounced than N-terminal unmodified ADan. The results were validated using conditioned media from cultivated HEK293 cells, which express APP variants favoring the formation of Aβ1-x, Aβ3-x or N-truncated pGlu-Aβ3-x species. Hence, we show that the ability of different amyloid peptides to impair synaptic function apparently correlates to their potential to form oligomers as a common mechanism. The pGlu-modification is apparently mediating a higher surface hydrophobicity, as shown by 1-anilinonaphtalene-8-sulfonate fluorescence, which enforces potential to interfere with neuronal physiology.

Keywords: Aβ, ABri, ADan, Alzheimer's disease, amyloid, pyroglutamate.

J. Neurochem. (2012) 10.1111/j.1471-4159.2012.07707.x

The aggregation and deposition of various amyloid-β protein (Aβ) species in brain is a hallmark of Alzheimer's disease (AD). Aβ is released from amyloid precursor protein (APP) by consecutive cleavage of β-secretase and γ-secretase, generating the N- and C-terminus of Aβ, respectively. The proteolytic events result primarily in formation of Aβ1-40, to lower extent in Aβ1-42 and Aβ1-38. Accumulation of Aβ42 precedes that of Aβ40 but later on in AD progression Aβ40 becomes a significant species in deposits (Iwatsubo *et al.* 1994). Besides its well characterized C-terminal heterogeneity, also N-terminally modified Aβ peptides have been reported. Among those, species are generated which are modified at position 3 or 11 by pyroglutamic acid

Received October 6, 2011; revised manuscript received January 19, 2012; accepted February 16, 2012.

Address correspondence and reprint requests to Dr. Stephan Schilling, Probiodrug AG, Weinbergweg 22, 06120 Halle, Germany.
E-mail: stephan.schilling@probiodrug.de

Abbreviations used: Aβ, amyloid-β protein; ACSF, artificial cerebrospinal fluid; AD, Alzheimer's disease; ANS, 1-anilinonaphtalene-8-sulfonate; APP, amyloid-β precursor protein; fEPSP, excitatory post-synaptic field potential; FBD, familial British Dementia; FDD, familial Danish Dementia; HFIP, 1,1,1,3,3,3-hexafluoro-2-propanol; LTP, long-term potentiation; MES, 2-(N-morpholino)ethanesulfonic acid; MTA buffer, MES/Tris/acetate buffer; PAGE, polyacrylamide gel electrophoresis; PICUP, photo-induced cross-linking of unmodified peptides; Ru(Bpy), tris(2,2′-bipyridyl)dichlororuthenium(II); ThT, thioflavin T.

(pGlu). The deposition of N-terminally truncated and modified Aβ progresses during development of AD in contrast to normal aging. This has been shown for late onset sporadic AD as well as for familial AD cases associated with mutations in the presenilin 1 gene (Russo *et al.* 2000; Miravalle *et al.* 2005; Piccini *et al.* 2005; Güntert *et al.* 2006).

In previous studies, a prominent influence of the pGlu-modification on the pH-dependent solubility, aggregation propensity and fibril morphology of Aβ has been reported (Schilling *et al.* 2006; Schlenzig *et al.* 2009). Compared with full-length Aβ, solubility of pGlu-modified Aβ is reduced at physiological pH, which, in turn, increases the aggregation propensity. In contrast to Aβ1-40 fibrils, those of pGlu-modified Aβ40 are shorter and frequently arranged in bundles. A similar impact of the N-terminal pGlu modification was observed for the aggregation of the amyloid peptide ADan. ADan and ABri are the main components of amyloid deposits in hereditary FDD and FBD. These forms of dementia are very similar to AD with regard to brain histopathology. pGlu-modified amyloid accounts for the majority of the deposits in FDD and FBD (Ghiso *et al.* 2001). Also with ADan and ABri, we showed that the pGlu residue reduces the solubility and increases the aggregation propensity (Schlenzig *et al.* 2009).

Compelling evidence suggests a role of pre-fibrillar oligomers and potentially diffusible protofibrils in synaptotoxicity. To further address the influence of the N-terminus of Aβ and ADan on the oligomer formation and toxicity, we aimed at a characterization of the smaller aggregates and their impact on synaptic plasticity. The results should further clarify the potential role of N-terminal heterogeneity in amyloid peptides for the development and progression of different neurodegenerative disorders.

Materials and methods

Materials

Amyloid peptides were synthesized as described in the next section. All chemicals were of analytical grade.

Synthesis of amyloid peptides

Peptides were synthesized in 50 μmol scale on an automated Symphony synthesizer (Rainin) using Fmoc-strategy. Synthesis of ADan and pGlu-ADan was described previously (Schlenzig *et al.* 2009). Briefly, Fmoc-Tyr(tBu)-NovaSyn ®TGA resin (Merck KGaA, Darmstadt, Germany) was used as starting material. After deprotection and purification by RP-HPLC, the disulfide bond was introduced by iodine oxidation. Crude peptides were dissolved in AcOH/H_2O (4 : 1) to a final concentration of about 2 mg/mL. After addition of 10 equivalents of iodine the solution was stirred at 22°C for 1 h. Completion of the oxidation was followed by HPLC and MALDI-TOF mass spectrometry. The reaction was quenched by addition of water and the iodine was extracted with tetrachloromethane. The aqueous phase was lyophilized and purified on a 250 × 21 mm Luna C18 column (Phenomenex, Aschaffenburg, Germany) using a gradient of acetonitrile in water (0.04% trifluoroacetic acid).

For synthesis of Aβx-37, Aβx-38 and Aβx-40 the corresponding pre-loaded Fmoc-AA-NovaSyn ®TGA resins (Merck KGaA) were used. Gly-25 and Ser-26 were incorporated using the pseudoproline unit Fmoc-Gly-Ser($\psi^{Me,Me}$ Pro)-OH (Merck Biosciences). After deprotection, the crude peptides were purified on a 250 × 21 mm Luna C18 column using a gradient of acetonitrile in water (0.04% trifluoroacetic acid).

Aβx-42 was synthesized on Fmoc-Ala-NovaSyn ®TGA resin (Merck Biosciences). Gly-25 and Ser-26 were incorporated using isoacyl dipeptide Boc-Ser(Fmoc-Gly)-OH (4 eq.). It was coupled with HOBt (4 eq.)/N,N′-diisopropylcarbodiimid (4.4 eq.) for 2 × 45 min. The resulting 26-*O*-isoacyl-β-amyloid(x-42) was purified after deprotection by RP-HPLC. Subsequently, the depsipeptides were dissolved in 0.1 M ammonium bicarbonate (pH 7.4) for 1 h to initiate isoacyl conversion. The reaction was monitored by analytical RP-HPLC. Analytical HPLC analysis was performed on a 4.6 × 150 mm Source 5RPC column (5 μm; GE Healthcare, Bucks, GB) with a gradient made of solvent A (0.1% NH_4OH in H_2O at pH 9) and solvent B (acetonitrile/solvent A 60 : 40).

In case of all N-terminal pyroglutamated peptides the pGlu was incorporated as Boc-pGlu-OH.

ThioflavinT assay

The thioflavinT (ThT) assay was carried out as described previously (Schlenzig *et al.* 2009). Briefly, all peptides were disaggregated in 1,1,1,3,3,3-hexafluoro-2-propanol (HFIP; Sigma, St Louis, MO, USA) and their concentration was determined spectrophotometrically. HFIP was evaporated and peptides were dissolved in 0.1 M NaOH. The peptides were diluted using a three-buffer system consisting of 2-(N-morpholino)ethanesulfonic acid (MES)/Tris/acetate, 50/100/50 mM, pH 8.0 according to Ellis and Morrison (1982). The buffer provides a constant ionic strength over a broad pH range. If required, the pH was adjusted using 0.1 M HCl. The peptide solution was diluted 2 : 1 using 40 μM ThT in water (final ThT concentration 20 μM, containing 0.05% sodium azide). The peptide concentration in the assay (200 μL) was 25 μM of Aβ37, Aβ38 and Aβ40 species. Aβ42 species, ADan and pGlu-ADan were applied in concentrations of 5 μM. Only samples of Aβ42 contained 5% HFIP. The plate was covered by an adhesive film, incubated in a plate reader at 37°C and the ThT fluorescence recorded for up to 2 weeks (excitation 440 nm, emission 490 nm). For each peptide, measurements were performed in six cavities of one plate. Data were normalized using GraphPad Prism 4 Software. The first value in each data set was defined 0% and the largest value was defined 100%.

Photo-induced cross-linking of unmodified peptides

Photo-induced cross-linking of unmodified peptides (PICUP) chemistry was performed, essentially as described by Bitan *et al.* (2003). Here, a freshly dissolved 50 μM peptide solution in 10 mM sodium phosphate buffer (pH 7.5) was incubated for 30 min at 22°C. Afterwards, 36 μL were substituted with 2 μL of 1 mM Ru(Bpy) and 2 μL 20 mM of ammonium persulfate, both in 10 mM phosphate buffer. The cross-linking was initiated by a beam of visible light for 2 s and quenched by the addition of 40 μL 2-fold reducing sample

buffer (Invitrogen, Carlsbad, CA, USA). Samples were analyzed by sodium dodecyl sulfate–polyacrylamide gel electrophoresis (PAGE) using a 10–20% Tris–Tricine gel (Invitrogen) followed by silver staining (Pierce, Rockford, IL, USA).

Transmission electron microscopy

Samples were taken from freshly dissolved peptides and applied to Formvar-coated copper grids (Plano GmbH, Wetzlar, Germany), incubated for 60 s, washed three times with water and subjected to negative staining using 1% uranyl acetate. Images were taken with an EM 900 (Carl Zeiss SMT, Oberkochen, Germany) operating at 80 kV using a Variospeed SSCCD camera SM-1k-120 (TRS, Moorenweis, Germany).

Measurement of ANS fluorescence

Fluorescence of 1-anilinonaphtalene 8-sulfonate (ANS, 200 μM) in MES/Tris/acetate buffer (25/50/25 mM, pH 8.0) added to Aβ species (25 μM) was measured after an incubation time of 40 min at 37°C. Excitation was 350 nm and emission was scanned from 400 to 650 nm on a Fluorimeter LS 50 B (Perkin Elmer, Waltham, MA, USA).

Long-term potentiation

For measuring the influence of various Aβ species, ADan and pGlu-ADan on long-term potentiation (LTP) acutely isolated hippocampal slices (400 μm thickness) were prepared from 4-month-old male C57Bl/6 mice (breeding stock of the Leibniz Institute for Neurobiology) as described previously (Rönicke *et al.* 2011). After decapitation both hippocampi were isolated and transverse hippocampal slices were prepared using a tissue chopper with a cooled stage. The slices were maintained in a pre-chamber containing 8 mL permanently carbogen-gasified artificial CSF (ACSF, 124 mM NaCl, 25.6 mM $NaHCO_3$, 1.2 mM KH_2PO_4, 4.9 mM KCl, 2.5 mM $CaCl_2$, 2 mM $MgSO_4$, 10 mM glucose) to allow peptide or the respective solvent control application for 2 h. HFIP-treated peptides (as described for the ThT assay) were dissolved in dimethylsulfoxide (Sigma) to a concentration of 50 μM, sonicated and immediately added to the ACSF containing pre-chamber at final concentrations of 500 or 250 nM. After treatment with peptides, the slices were transferred into a submerged-type recording chamber, where they recovered for at least 30 min before starting with the electrophysiological experiments. The recording chamber was constantly perfused with ACSF at a rate of 2.5 mL/min at 33 ± 1°C. Synaptic responses were elicited by stimulation of the Schaffer collateral–commissural fibers in the stratum radiatum (CA1 region) by using lacquer coated stimulating electrodes of stainless steel. Field excitatory post-synaptic potentials (fEPSP) were recorded with glass electrodes (filled with ACSF, 14 MΩ) that were placed in the apical dendritic layer. The initial slope of the fEPSP was used as measure of this potential. The stimulus strength of the test pulses was adjusted to 30% of the fEPSP slope maximum. During baseline recording single stimuli were applied every minute. Once a stable baseline had been established, long-term potentiation was induced by applying three series of strong tetanus pulses. The interval between the three series was 10 min. Each series consisted of hundred 0.2 ms pulses at 10-ms intervals.

For measuring the influence of Aβ-conditioned medium on LTP, acute isolated slices from rats were prepared basically as described (Rönicke *et al.* 2009). Seven- to 8-week-old male Wistar rats (Harlan Laboratories, Borchen, Germany) were decapitated, their brains quickly removed and placed into ice-cold ACSF having the same composition as described above. Both hippocampi were isolated and transverse hippocampal slices (400 μM thickness) were prepared. The slices were maintained in a pre-chamber containing 8 mL permanently carbogen-gasified Aβ-conditioned medium (total Aβ 3 ng/mL, approximately 700 nM) or control medium for 2 h. Then, slices were placed into an interface recording chamber and were allowed to recover for at least 1 h. The chamber was constantly perfused with Ringer solution at a rate of 1 mL/min. The surface of the slices was exposed to a moist carbogen atmosphere, which was exchanged at a rate of 20 L/h. The temperature of the chamber was maintained at 34 ± 1°C. Synaptic responses were elicited by stimulation of the Schaffer collateral–commissural fibers in the stratum radiatum (CA1 region) basically as described above, but during baseline recording three single stimuli (10-s interval) were averaged every 5 min.

Preparation and analysis of conditioned media

Human embryonic kidney cells (HEK293) were cultured in Dulbecco′s modified eagle medium supplemented with 10% fetal bovine serum and Gentamycin in a humidified atmosphere of 5% CO_2 at 37°C. Cells were seeded into 75 cm^2 flasks and transfected the next day with vectors APP-NL, APP-NLE, APP-NLQ (Shirotani *et al.* 2002; Cynis *et al.* 2008) and pcDNA3.1 for control using Lipofectamin2000 (Invitrogen) according to the manufacturer's guidelines. The medium was exchanged with Dulbecco′s modified eagle medium without phenol red, fetal bovine serum and Gentamycin 24 h later. After additional 20 h the supernatant was collected and centrifuged at 1 000 *g* for 5 min to remove remaining cells. Samples were taken for Aβ ELISA, immunoprecipitation and size exclusion chromatography (SEC) and the remaining medium was readily frozen at −80°C until use. Before incubating the slices, Aβ concentration was determined by specific sandwich ELISA detecting total Aβx-40 (IBL-International, Hamburg, Germany) and normalized to 3 ng/mL by the addition of conditioned medium. After immunoprecipitation, the Aβ composition was analyzed using western blot, applying 15% urea–PAGE gels according to Klafki *et al.* (1996).

To investigate the oligomeric state of Aβ, conditioned media were centrifuged to remove insoluble material at 13 000 *g* for 15 min and subjected to size exclusion chromatography on a Superdex 75 10/300 column (GE Healthcare, Bucks, GB). The mobile phase consisted of 50 mM Tris, 100 mM NaCl, pH 8.0. 250 μL were injected, fractions of 1 mL collected and the concentration of Aβ determined by ELISA.

Results

Fibril formation of Aβ and ADan peptides

In our previous investigations, we characterized the formation of fibrils from N-truncated and pGlu-modified Aβ40 peptides (Schilling *et al.* 2006; Schlenzig *et al.* 2009). In these studies, the peptides exhibited enhanced aggregation propensity due to truncation and modification of their N-termini. Here, we aimed at a characterization of the role of the pGlu-modification for the aggregation propensity of other C-terminal

variants of Aβ, that is, Aβ37, Aβ38 and Aβ42. The isoelectric point of the peptides and thus the pH value has been shown to exert a significant influence on the solubility of peptides, as shown previously for Aβ40. Because a C-terminal truncation does not change the theoretical pI of the Aβ variants (Aβ1-37/38/40/42 pI = 5.43; pGlu-Aβ3-37/38/40/42 pI = 6.62; ADan pI = 6.49; pGlu-ADan pI = 6.95; pI calculated with peptide property calculator from GenScript, using an acetylated amino acid to mimic pGlu; https://www.genscript.com/ssl-bin/site2/peptide_calculation.cgi), we characterized the aggregation of the peptides at pH 8.0, a pH which is fairly distant from the pI of all amyloid peptides analyzed.

The fibril formation from Aβ1-40 required a long lag time of about 150–200 h, that of Aβ3-40 even longer (about 400 h, Figure S1a). In contrast, as observed previously the incubation of monomeric pGlu-Aβ3-40 caused a significantly accelerated aggregation (Fig. 1a). Interestingly, a C-terminal truncation by two amino acids did not reduce the aggregation propensity. The characteristic exponential fibril growth was observed with Aβ1-38 after about 100 h incubation time (Fig. 1b). Again, the N-terminal pGlu-modification decreased the lag phase. Furthermore, C-terminal truncation resulting in Aβx-37 did not have a significant effect on aggregation propensity, but similar to the other Aβ species, pGlu-Aβ3-37 aggregated faster than Aβ1-37 (Fig. 1c). A decline of the ThT signal was observed with pGlu-Aβ3-40 and pGlu-Aβ3-37 at the end of the period of investigation. Such a phenomenon was previously attributed to formation of higher ordered, suprafibrillar assemblies (Walsh *et al.* 2001). The electron microscopic images indeed support different morphologies of pGlu-Aβ and Aβ1-x fibrils. We found mainly smooth fibrils in case of Aβ1-x but shorter fibrils that strongly tend to form lateral interactions for pGlu-Aβ3-x species (images are displayed in Fig. 1).

In contrast to the C-terminally truncated peptides, both Aβ42-derivatives displayed fibril formation within a few hours. As the rapid formation did not allow a reliable observation of a lag-phase (Figure S1b), we added 5% HFIP to tune down the β-sheet formation to both reactions. Although the relative difference in the lag phase was not as substantial as for the C-terminally truncated peptides, pGlu-Aβ3-42 showed again accelerated fibril formation (Fig. 1d).

Finally, we characterized the *in vitro* fibril formation of ADan and pGlu-ADan (Fig. 1e). An exponential increase of fluorescence intensity was observed with pGlu-ADan. In contrast, we did not observe a significant change of fluorescence intensity with ADan under these conditions, implying slow aggregation. Only few fibrils could be found after 10 days of incubation.

Thus, the formation of larger aggregates of all peptides is influenced by the N-terminal amino acid in a similar manner, although the degree of acceleration by N-terminal pGlu differs between the amyloid species.

Oligomer formation – PICUP

As the assembly of amyloid peptides into fibrillar aggregates, which are detected by ThT-fluorescence, represents a seeded process, we aimed at a characterization of the formation of oligomers. To investigate potential differences we applied PICUP. PICUP enables visualization of small oligomers like dimers, trimers and tetramers that are usually unstable in sodium dodecyl sulfate–PAGE (Bitan *et al.* 2003). Using the method, two populations of oligomers are obtained. One population is due to stochastic formation controlled by diffusion processes and one is caused by cross-linking of preformed oligomers that are in a dynamic equilibrium within the incubation solution. To investigate the early events during the aggregation process, the cross-linking was performed directly after dissolution of the monomeric peptides.

Applying PICUP to various Aβ species, we obtained a similar pattern of oligomer ladders with Aβ1-37, Aβ1-38 and Aβ1-40 with a slightly pronounced band corresponding to trimers (Fig. 2a; first lanes). The respective N-terminally truncated Aβ3-x species showed a very similar pattern (Figure S2). For pGlu-Aβ3-37, pGlu-Aβ3-38 and pGlu-Aβ3-40, however, remarkable differences could be observed. Here, the band of trimers is pronounced and significantly broadened (Fig. 2a, second lanes). Such an oligomeric pattern was also observed, if low molecular weight fractions of Aβ after size-exclusion chromatography were applied to cross-linking, as exemplarily shown for Aβ1-40 and pGlu-Aβ3-40 in Fig. 2c. Thus, the oligomers were not preformed, but rather rapidly generated in aqueous solution. In contrast to Aβ1-37/38/40, PICUP analysis of Aβ1-42 and pGlu-Aβ3-42 revealed a significant fixation of trimers and tetramers (Fig. 2a). A densitometric analysis highlights the intense bands of pGlu-Aβ3-x trimers/tetramers, which appears similar to Aβ1-42/pGlu-Aβ3-42 (Fig. 2b).

The cross-linking of ADan and in particular of pGlu-ADan led to fixation of oligomers with higher molecular weight. Both peptides apparently formed pentamers/hexamers. However, the bands are more intense with pGlu-ADan than with ADan, which appeared diffuse (Fig. 2a). In addition, we observed a strong signal for large oligomeric forms of pGlu-ADan. These higher aggregates hardly entered the separation gel.

Transmission electron microscopic analysis of oligomers

To further substantiate the differences observed in PICUP analysis, we assessed Aβ38, Aβ40, Aβ42 and ADan in electron microscopy. Comparing the electron micrographs of freshly dissolved Aβ1-38/40 and pGlu-Aβ3-38/40, clear differences are observed depending on the N-terminus of the peptides (Fig. 3). Aβ1-38 and Aβ1-40 form very small structures (Fig. 3a and c) whereas pGlu-Aβ3-38 and pGlu-Aβ3-40 form larger conglomerates (Fig. 3a and d). Similarly, rather globular aggregates were observed with pGlu-Aβ3-42 (Fig. 3f). In contrast, early oligomers of Aβ1-42 have a more wormlike appearance (Fig. 3e). Thus, although the size of

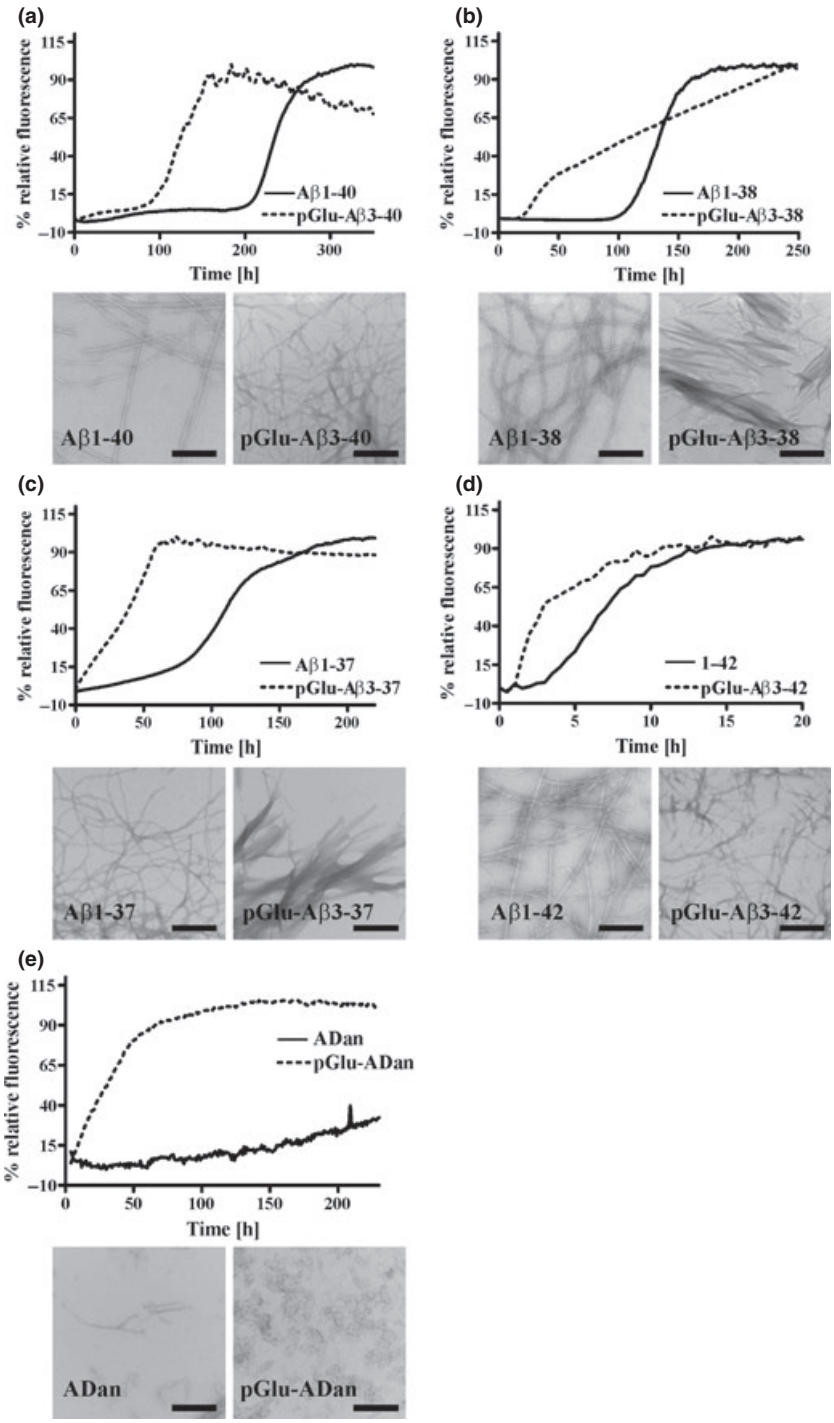

Fig. 1 Aggregation kinetics of different Aβ and ADan species, monitored by ThT-fluorescence. The diagrams correspond to: Aβ40 (a), Aβ38 (b), Aβ37 (c), Aβ42 (d) and ADan (e). In addition, electron micrographs of the fibrillar aggregates are provided. The concentration of Aβ40, Aβ38 and Aβ37 was 25 μM, whereas the concentration of Aβ42 and ADan was 5 μM (ThT 10 μM, 0.05% sodium azide). Samples of Aβ42 contained 5% HFIP. Measurements were performed as 6 replicates and data were normalized to 100%. All reactions were carried out at pH 8.0 and 37°C. Bars in micrographs indicate 200 nm; magnification was 50 000×. For all amyloid peptides investigated, the N-terminal pGlu-modification leads to an acceleration of aggregation compared with non-modified peptides. Furthermore, fibrils of pGlu-modified amyloid peptides are shorter and strongly tend to form lateral interactions.

the oligomers is not reliably obtained by our transmission electron microscopic analysis, substantial differences between Aβ peptides are also observed without chemical cross-linking, further supporting rapid aggregation if the N-terminus is truncated and pGlu-modified.

The shape of the oligomeric forms of ADan and pGlu-ADan was rather similar to each other (Fig. 3g and h). The main difference appeared to be that the pGlu-peptide formed aggregates of larger size, which mirrors the observations from the PICUP analysis.

Analysis of ANS fluorescence

To compare the apolar nature of unmodified versus pGlu-modified Aβ, changes in fluorescence of ANS as a measure of surface hydrophobicity (Cardamone and Puri 1992) was investigated. In general, the ANS fluorescence intensity is

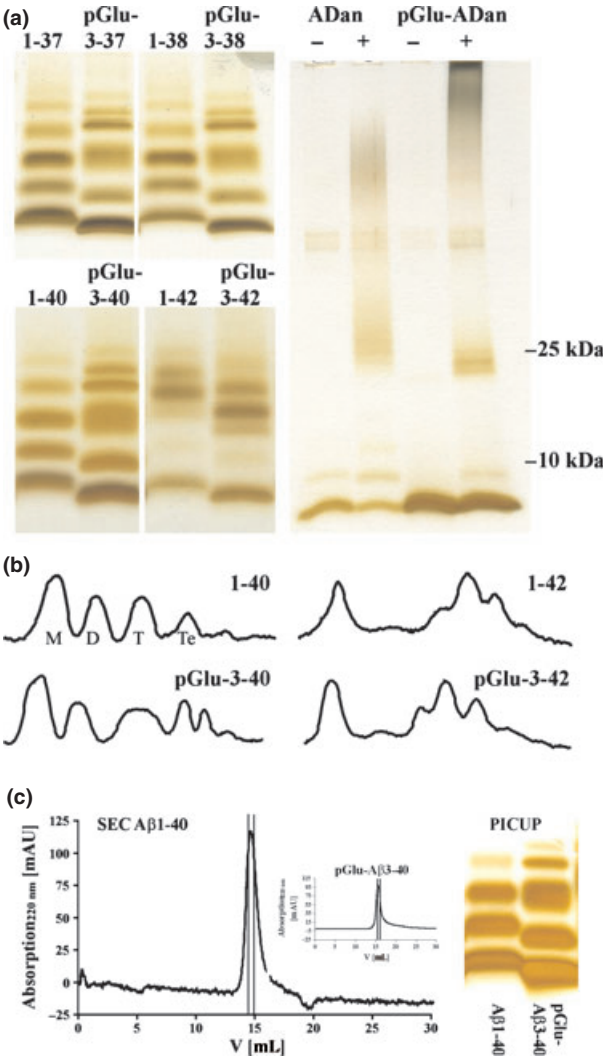

Fig. 2 (a) SDS–PAGE analysis of Aβ37, Aβ38, Aβ40, Aβ42 and ADan following photo-induced cross-linking of the unmodified peptides (PICUP). For Aβ, the first lane in each picture corresponds to the full-length species (Aβ1-x), whereas the second lane contains the respective pGlu-modified peptide (pGlu-Aβ3-x). In case of ADan, non-cross-linked (–) and cross-linked (+) peptide preparations are compared. A densitometric analysis of the band pattern of Aβ40 and Aβ42 is provided in panel (b); (M-monomer, D-dimer, T-trimer, Te-tetramer). The results of the PICUP analysis did not differ if Aβ was separated by size exclusion chromatography prior to cross-linking, as shown for Aβ1-40 and pGlu-Aβ3-40 (c). All products were analyzed by 10–20% Tris–Tricine gel electrophoresis and visualized by silver staining. The pGlu-modification significantly enforces the formation of small oligomers from Aβ37, Aβ38 and Aβ40. The effect is not obvious with Aβ42. Differences are also observed with pGlu-ADan, although these aggregates appear much larger compared with the Aβ oligomers detected.

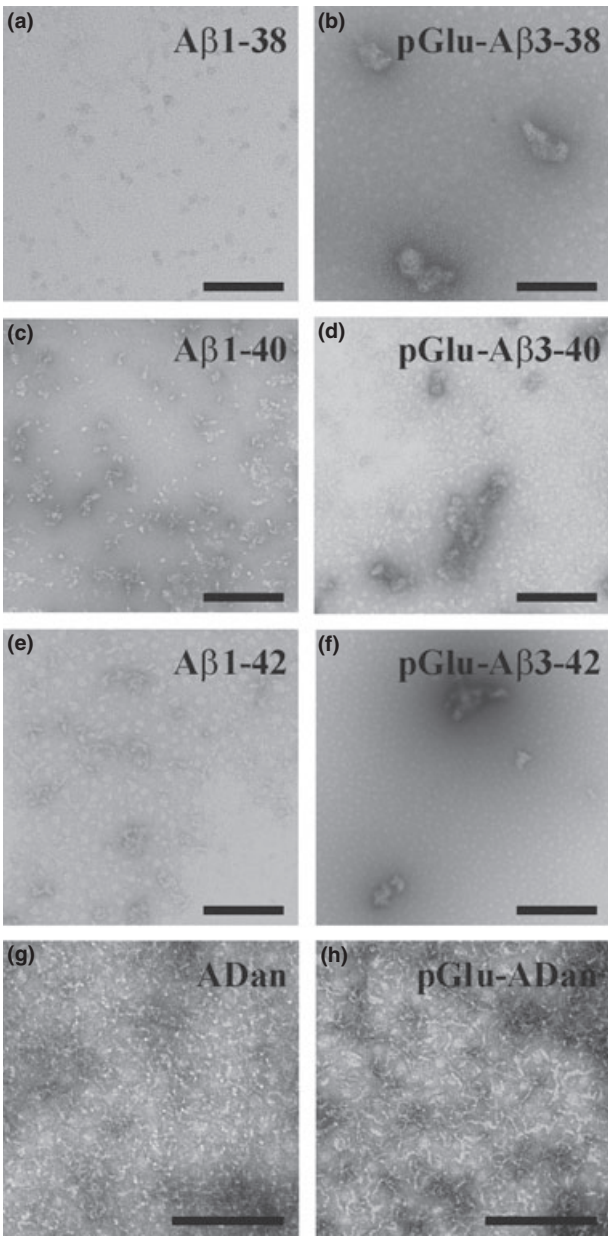

Fig. 3 Electron micrographs of small aggregates of amyloid peptides Aβ1-38 (a), pGlu-Aβ3-38 (b), Aβ1-40 (c), pGlu-Aβ3-40 (d), Aβ1-42 (e), pGlu-Aβ3-42 (f), ADan (g) and pGlu-ADan (h). Aβ38, Aβ40 (25 μM) and Aβ42 (5 μM) were dissolved in 10 mM sodium phosphate buffer, pH 7.5 and incubated for 30 min. ADan peptides (25 μM) were dissolved in MTA-buffer pH 4.0. In contrast to N-terminally unmodified Aβ, the pGlu-modified Aβ species form larger, globular oligomeric aggregates. ADan and pGlu-ADan associate into worm-like aggregates, which appear larger for the pGlu-modified peptide species, supporting the observations from PICUP analysis. Bars in micrographs indicate 200 nm; magnification was 50 000× or 85 000×.

lower in the presence of C-terminally truncated Aβx-40 compared with Aβx-42 (Fig. 4). In particular, freshly dissolved Aβ1-40 and Aβ3-40 (Figure S3) do not have any effect on ANS fluorescence. The pGlu-modified Aβ shows a significantly stronger influence on the fluorescence intensity of ANS and results in a shift of maximum emission from 519

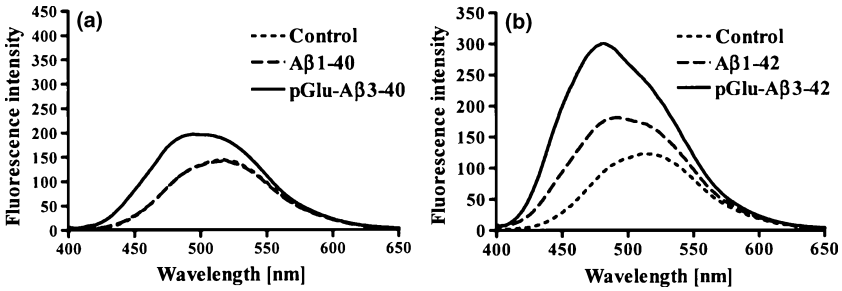

Fig. 4 Influence of Aβ on fluorescence intensity of ANS. Peptide concentration was 25 μM in MES/Tris/acetate buffer pH 8.0, 200 μM ANS. Peptides were incubated at 37°C for 40 min prior to measurement. pGlu-Aβ3-40 has an increasing influence on fluorescence intensity of ANS, whereas fluorescence curves of control and Aβ1-40 appear identical (a). Aβ1-42 and pGlu-Aβ3-42 increase fluorescence intensity of ANS. Compared with Aβ1-42, pGlu-Aβ3-42 triggered a fluorescence increase which appeared twofold stronger and further blue-shifted (b).

to 480 nm, suggesting a fast formation of aggregates with a more hydrophobic surface.

Influence of synthetic Aβ and ADan on hippocampal LTP

To address the functional consequences of the different oligomers formed from Aβ and ADan and their truncated and pGlu-modified counterparts, we assessed the influence of the Aβ38, Aβ40, Aβ42 and ADan peptides on long-term potentiation of synaptic response in hippocampal slices from mice. Here, freshly dissolved Aβ1-38, Aβ1-40 (Fig. 5a and c) and Aβ3-40 (Figure S4) did not show any effect on synaptic function at a concentration of 500 nM. In contrast, pGlu-Aβ3-38 and pGlu-Aβ3-40 both significantly impaired the LTP at that concentration (Fig. 5b and d). Thus, apparently, the accelerated aggregation mediated by the N-terminus (compare Figs 1 and 2) leads to a rapid generation of ANS fluorescence effecting oligomers which impair the neuronal function.

In accordance with this interpretation, Aβ1-42 and pGlu-Aβ3-42 impaired hippocampal LTP (Fig. 6a and b, insets) at a concentration of 500 nM. A lower Aβ concentration revealed a higher activity of pGlu-Aβ3-42 to affect potentiation. Thus, the N-terminus of Aβ42 clearly influences the synaptotoxic potential at lower concentration.

Finally, we also assessed the influence of the amyloidogenic peptides ADan and pGlu-ADan on hippocampal LTP. Interestingly, pGlu-ADan impaired the potentiation in a similar concentration as the Aβ peptides applied at 500 nM. However, the reduction in LTP caused by the non-modified ADan peptide did not reach statistical significance (Fig. 6c and d).

Influence of cell-born Aβ on hippocampal LTP

To substantiate the findings obtained with synthetic Aβ we collected conditioned media from HEK293 cells which secrete primarily Aβ1-40, Aβ3-40 or pGlu-Aβ3-40

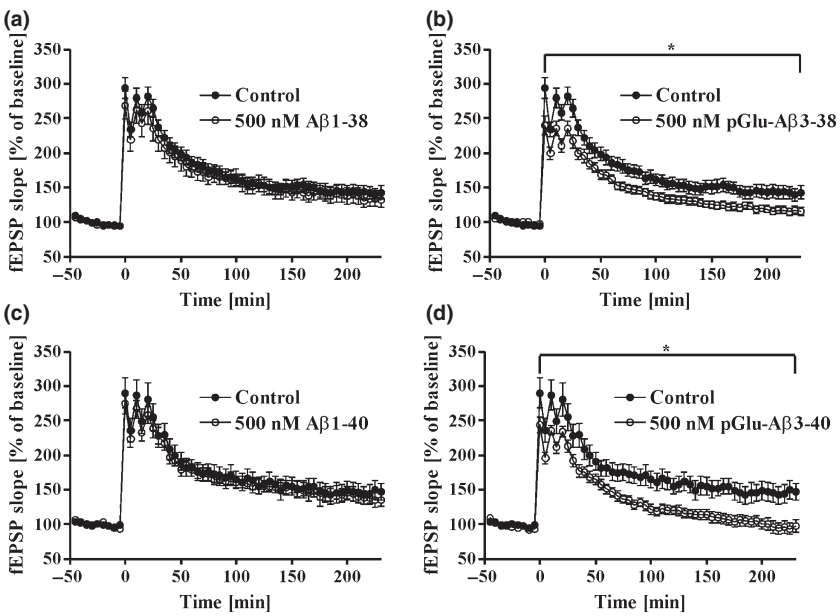

Fig. 5 Influence of freshly dissolved Aβ1-38 (a), pGlu-Aβ3-38 (b), Aβ1-40 (c) and pGlu-Aβ3-40 (d) on long-term potentiation (LTP) in acute hippocampal slices from mice. The amyloid peptides were dissolved in DMSO and diluted in ACSF to a final concentration of 500 nM, controls did not contain the peptide. In accordance with the observation of oligomers, only pGlu-Aβ3-38 and pGlu-Aβ3-40 impaired the neuronal physiology. For experimental details, see Methods (control: $n \geq 17$, peptide: $n \geq 12$, $^*p \leq 0.05$ ANOVA with repeated measures).

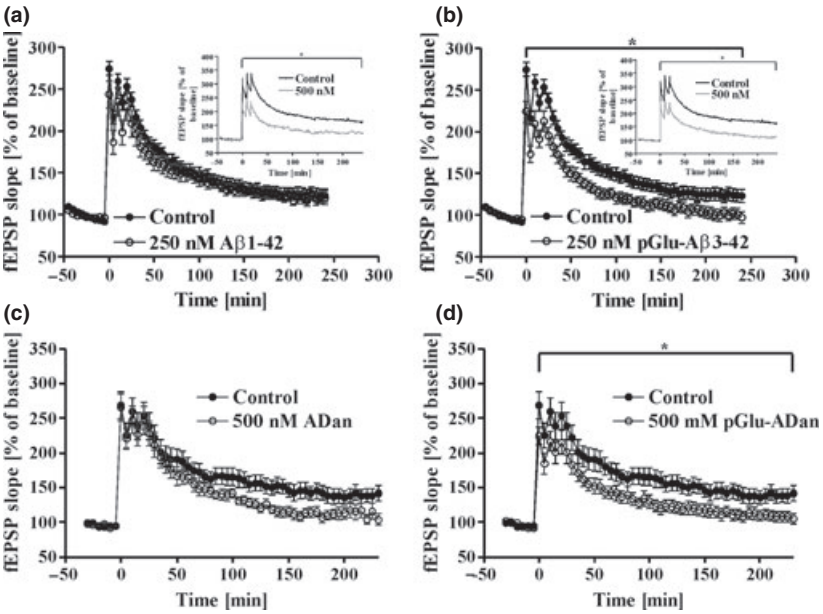

Fig. 6 Influence of Aβ1-42 (a), pGlu-Aβ3-42 (b), ADan (c) and pGlu-ADan (d) LTP in hippocampal slices from mice. In contrast to Aβ38 and Aβ40, Aβ1-42 and pGlu-Aβ3-42 significantly impaired LTP at a concentration of 500 nM (Insets). At lower concentration (250 nM) only N-terminal pGlu-modified Aβ42 (b) decreased synaptic response. Likewise, pGlu-modified ADan (d) impaired LTP. A tendency to impairment of LTP was also observed with ADan (c), however, the effect did not reach statistical significance. For experimental details, see Methods (control: $n \geq 17$, peptide: $n \geq 12$, $^*p \leq 0.05$ ANOVA with repeated measures).

(Shirotani *et al.* 2002). The cells were transfected with various APP constructs that favor the formation of either of the three Aβ species. The APP-NL construct contains the Swedish and London mutation. As a result, the cells mainly secrete Aβ1-40/42. The APP-NLE additionally includes a deletion of the first two amino acids of Aβ. Furthermore, in APP-NLQ amino acid 3 of Aβ is substituted by glutamine (E599Q). These modifications of APP result in the secretion of Aβ3-40/42 and pGlu-Aβ3-40/42, respectively (Figure S5). Application of the conditioned media from APP-NLE and APP-NL (containing primarily Aβ3-40 and Aβ1-40, respectively) to hippocampal slices revealed a non-significant influence on the synaptic function (Fig. 7). The tendency in reduction of LTP is most likely caused by the Aβ3-42 and Aβ1-42 peptides generated by the transfected cells and released to the culture medium. In accordance with the previous findings, a treatment of slices with conditioned medium containing pGlu-Aβ3-40/42, which was obtained from APP-NLQ transfected cells, caused a significant disruption of LTP. A further analysis of the oligomeric state of the Aβ peptides within the media using size exclusion chromatography in combination with ELISA quantification revealed most of the Aβ being monomer/dimer. Only in case of APP-NLQ transfected cells, the medium contained soluble higher oligomeric Aβ eluting close to the void volume (Fig. 7b), illustrating the rapid oligomerization of pGlu-modified Aβ in cell-based conditions.

Discussion

In Alzheimer's disease accumulating evidence attributes cognitive deficits to so-called 'soluble oligomers' of amyloid β peptide (Lambert *et al.* 1998; Walsh and Selkoe 2004; Cleary *et al.* 2005; Walsh *et al.* 2005; Townsend *et al.* 2006). Notably, the appearance of Aβ oligomers rather correlates with the development of AD than the total amyloid burden in the brain (Shankar *et al.* 2008). Sub-micromolar concentrations of Aβ oligomers were frequently shown to have detrimental effects on brain cells, for example, impairment of synaptic function and induction of neuronal cell death whereby, the disruption of LTP is an early aspect reflecting the collapse of glutamatergic dendritic spines (Hsieh *et al.* 2006; Rönicke *et al.* 2011).

Aβ42 species which precede deposition of Aβ40 (Iwatsubo *et al.* 1994; Lemere *et al.* 1996), have been shown to potently affect the neuronal physiology (Murakami *et al.* 2003; Irie *et al.* 2005). A truncation of the C-terminus (Jarrett *et al.* 1993) leads to much slower aggregation and oligomer formation, which correlates with lower potential to affect long-term potentiation. Although there is compelling evidence for an oligomer-induced neurotoxicity, the actual composition of the oligomers exerting toxicity apparently varies and is still matter of further investigations. Species, which have been suggested to be particularly toxic range from dimers (Shankar *et al.* 2008) to trimers (Cleary *et al.* 2005) up to, for instance, larger diffusible globulomers (Lesne *et al.* 2006; Nimmrich *et al.* 2008). However, it is not unlikely that different Aβ oligomers co-exist *in vivo*. These might share common structural features, which mediate the toxic potential (Kayed *et al.* 2003).

Here, we show that an N-terminal pGlu-modification might account for rapid oligomer formation and oligomer-induced neurophysiological changes. In previous investigations, it has been shown that N-terminally truncated and modified forms of Aβ40 and Aβ42, in particular pGlu-Aβ3-x, show a decreased solubility and a significantly enhanced

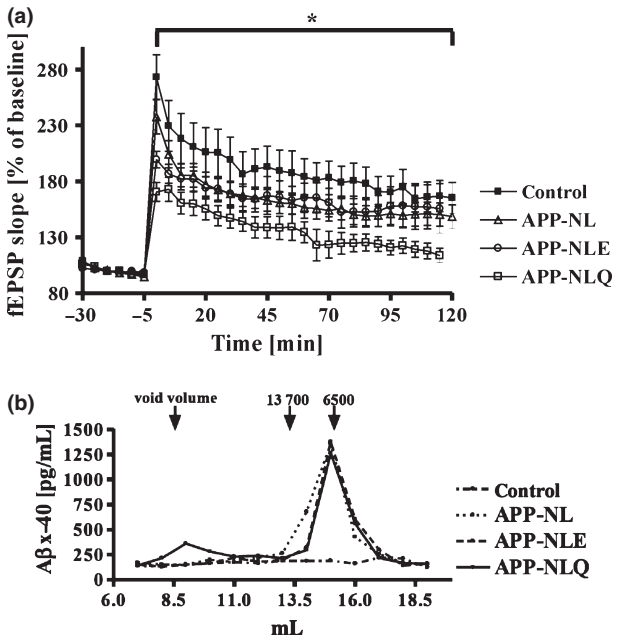

Fig. 7 Influence of conditioned media from transfected HEK293 cells on LTP (a) and oligomeric state of Aβ in these media (b). The conditioned media were collected after transient expression of the APP-forms APP-NL, APP-NLE and APP-NLQ, which results in secretion of Aβ1-x, Aβ3-x or pGlu-Aβ3-x into the medium (see Figure S5). Within the media, Aβ40 peptides represent the dominant form. The total Aβ concentration in the media did not differ substantially after transfection, slight differences where adjusted by dilution. (a) In accordance with the previous investigations, we observed a significant impairment of LTP with conditioned medium containing pGlu-Aβ3-x peptides (control: $n \geq 10$, peptides: $n \geq 12$, $^*p \leq 0.05$ ANOVA with repeated measures). (b) Two hundred and fifty microliters of conditioned media were fractionated by size exclusion chromatography (Superdex 75, 10/300) and concentration of Aβ in the fractions was analyzed by ELISA. Only the conditioned medium from APP-NLQ expressing cells contained detectable amounts of soluble oligomeric Aβ, which elutes close to the void volume of the column. Thus, pGlu-Aβ formation coincides with enforced formation of oligomeric Aβ in the cell-based system. Arrows with numbers indicate the elution of standard proteins (masses in Da).

propensity to aggregation (He and Barrow 1999; Schilling *et al.* 2006; D'Arrigo *et al.* 2009; Schlenzig *et al.* 2009). Our present study shows that N-terminal truncation and modification causes an accelerated aggregation into ThT-fluorescent conglomerates of Aβ37/38/40/42 and ADan in general (Fig. 1). In accordance with numerous studies from the literature, we found the highest propensity of Aβ42 to form such aggregates. Interestingly, those Aβ species which form fibrils most rapidly, give rise to instant formation of oligomers, as analyzed using PICUP chemistry and electron microscopy.

The PICUP pattern, however, differ between Aβ42 and its C-terminally truncated counterparts Aβ38 and Aβ40. While with Aβ42 species, that is, Aβ1-42 and pGlu-Aβ3-42, a prominent formation of trimers and tetramers can be concluded, the bands observed with pGlu-Aβ3-40 and pGlu-Aβ3-38 are less clearly defined and might correspond to trimers. In contrast, the PICUP and electron microscopic analysis of Aβ1-40 and Aβ1-38 did not provide a clear hint to rapid oligomer formation upon dissolution. Although the actual structure of the instantly formed oligomers from pGlu-Aβ3-40 and pGlu-Aβ3-38 appears to bear differences compared with Aβ42, the aggregates potently affect the neuronal physiology as investigated by hippocampal LTP. In accordance with the observation of oligomers in PICUP analysis, we only detected an influence of species on LTP, when a presence of oligomeric forms was observed in PICUP and when an increased hydrophobicity was concluded from the effect of the peptides on ANS fluorescence intensity. Moreover, the analysis of conditioned media from cultured cells clearly suggests that the effect is not limited to synthetic Aβ species but is intrinsically mediated by the N-terminal truncation and modification, even at lower concentrations and physiological mixtures of different Aβ forms as produced by transfected cells.

The presented data demonstrate clearly a direct influence of the N-terminal pGlu-modification of Aβ peptides on the velocity to form oligomers and their polar nature, which then apparently translates into an accelerated formation of larger aggregates with fibrillar characteristics. A typical property of these fibrils is that those share a bundled arrangement, potentially mediated by hydrophobic lateral interactions. The N-terminal truncation and pGlu-modification of Aβ leads to a loss of N-terminal charge, which has been suggested to result in a significant increase of hydrophobicity (D'Arrigo *et al.* 2009; Schlenzig *et al.* 2009). Interestingly, recent studies involving different amyloid species point to a crucial impact of oligomeric surface hydrophobicity on the neurotoxic potential (Bolognesi *et al.* 2010; Campioni *et al.* 2010). Likewise, the N-terminus-mediated oligomer formation of Aβ might provoke forms, which very potently mediate interaction with hydrophobic cell surfaces and receptors. Hence, the pGlu-modification basically increases hydrophobicity, which might be the main determinant for the pathogenic potency. Such a hypothesis is supported by our investigations of ADan, which provided similar results with regard to the influence of the pGlu-residue at the N-terminus. Again, the modification leads to an increase of the aggregation velocity, it impacts the fibrillar appearance and the oligomeric pattern in solution or conditioned medium, which in turn, massively affects the LTP as shown here for the first time.

Several lines of evidence suggest that the accumulation of N-terminally truncated and modified forms of Aβ correlate with the progression or severity of disease. For instance, presence of water-soluble pGlu-Aβ3-42 was linked to AD patients (Piccini *et al.* 2005) and pGlu-modified Aβ-species accumulated during progression of disease in human AD

deposits, in contrast to Aβ1-42 (Guntert *et al.* 2006). In addition, the inherited forms of AD caused by mutations in the presenilin genes are accompanied by very early and dominant appearance of truncated and modified forms of Aβ (Russo *et al.* 2000; Miravalle *et al.* 2005). Finally, attenuation of pGlu-Aβ formation has shown therapeutic efficacy in mouse models of AD (Schilling *et al.* 2008). Direct overexpression of pGlu-Aβ in a mouse model is accompanied by a severe injured phenotype and high lethality (Alexandru *et al.* 2011). The results presented here provide further evidence for a specific pathogenic role of pGlu-modified amyloid peptides, which links the accumulation of such species in AD, FBD and FDD to a potential pathophysiological function. Our observations might thus provide also implications for current treatment strategies, which primarily focus on reduction of total Aβ or more subtle of the Aβ1-42 formation and toxicity.

Acknowledgement

The work was supported by the Federal Ministry of Education and Science of Germany (BMBF), grant no. 0315223 to probiodrug AG (HUD).

Supporting information

Additional supporting information may be found in the online version of this article:

Figure S1. Aggregation kinetics of Aβx-40 (a) and Aβx-42 (b) at pH 8.0 and 37°C, monitored by ThT-fluorescence.

Figure S2. SDS–PAGE analysis of Aβ40, Aβ38 and Aβ37 following photo-induced cross-linking of unmodified peptides (PICUP), including Aβ3-x.

Figure S3. Influence of Aβx-40 on fluorescence intensity of ANS.

Figure S4. Influence of freshly dissolved Aβ3-40 on long-term potentiation (LTP) in acute hippocampal slices from mice.

Figure S5. Analysis of Aβ forms in conditioned media of HEK293 cells after transient transfection with APP constructs APP-NL, APP-NLE and APP-NLQ.

As a service to our authors and readers, this journal provides supporting information supplied by the authors. Such materials are peer reviewed and may be re-organised for online delivery, but are not copy-edited or typeset. Technical support issues arising from supporting information (other than missing files) should be addressed to the authors.

References

Alexandru A., Jagla W., Graubner S. *et al.* (2011) Neurotoxicity and lethal phenotype of pE3-Aβ expression in a transgenic mouse model – pE3-Aβ formation and neuronal loss in TBA2.1 mice. *J. Neurosci.* **31**, 12790–12801.

Bitan G., Kirkitadze M. D., Lomakin A., Vollers S. S., Benedek G. B. and Teplow D. B. (2003) Amyloid beta-protein (Abeta) assembly: Abeta 40 and Abeta 42 oligomerize through distinct pathways. *Proc. Natl Acad. Sci. USA* **100**, 330–335.

Bolognesi B., Kumita J. R., Barros T. P., Esbjorner E. K., Luheshi L. M., Crowther D. C., Wilson M. R., Dobson C. M., Favrin G. and Yerbury J. J. (2010) ANS binding reveals common features of cytotoxic amyloid species. *ACS Chem. Biol.* **5**, 735–740.

Campioni S., Mannini B., Zampagni M. *et al.* (2010) A causative link between the structure of aberrant protein oligomers and their toxicity. *Nat. Chem. Biol.* **6**, 140–147.

Cardamone M. and Puri N. K. (1992) Spectrofluorimetric assessment of the surface hydrophobicity of proteins. *Biochem. J.*, **282**(Pt 2), 589–593.

Cleary J. P., Walsh D. M., Hofmeister J. J., Shankar G. M., Kuskowski M. A., Selkoe D. J. and Ashe K. H. (2005) Natural oligomers of the amyloid-beta protein specifically disrupt cognitive function. *Nat. Neurosci.* **8**, 79–84.

Cynis H., Scheel E., Saido T. C., Schilling S. and Demuth H. U. (2008) Amyloidogenic processing of amyloid precursor protein: evidence of a pivotal role of glutaminyl cyclase in generation of pyroglutamate-modified amyloid-beta. *Biochemistry* **47**, 7405–7413.

D'Arrigo C., Tabaton M. and Perico A. (2009) N-terminal truncated pyroglutamyl beta amyloid peptide Abetapy3-42 shows a faster aggregation kinetics than the full-length Abeta1-42. *Biopolymers* **91**, 861–873.

Ellis K. J. and Morrison J. F. (1982) Buffers of constant ionic strength for studying pH-dependent processes. *Methods Enzymol.* **87**, 405–426.

Ghiso J., Revesz T., Holton J. *et al.* (2001) Chromosome 13 dementia syndromes as models of neurodegeneration. *Amyloid* **8**, 277–284.

Güntert A., Dobeli H. and Bohrmann B. (2006) High sensitivity analysis of amyloid-beta peptide composition in amyloid deposits from human and PS2APP mouse brain. *Neuroscience* **143**, 461–475.

He W. and Barrow C. J. (1999) The A beta 3-pyroglutamyl and 11-pyroglutamyl peptides found in senile plaque have greater beta-sheet forming and aggregation propensities in vitro than full-length A beta. *Biochemistry* **38**, 10871–10877.

Hsieh H., Boehm J., Sato C., Iwatsubo T., Tomita T., Sisodia S. and Malinow R. (2006) AMPAR removal underlies Abeta-induced synaptic depression and dendritic spine loss. *Neuron* **52**, 831–843.

Irie K., Murakami K., Masuda Y., Morimoto A., Ohigashi H., Ohashi R., Takegoshi K., Nagao M., Shimizu T. and Shirasawa T. (2005) Structure of beta-amyloid fibrils and its relevance to their neurotoxicity: implications for the pathogenesis of Alzheimer's disease. *J. Biosci. Bioeng.* **99**, 437–447.

Iwatsubo T., Odaka A., Suzuki N., Mizusawa H., Nukina N. and Ihara Y. (1994) Visualization of A beta 42(43) and A beta 40 in senile plaques with end-specific A beta monoclonals: evidence that an initially deposited species is A beta 42(43). *Neuron*, **13**, 45–53.

Jarrett J. T., Berger E. P. and Lansbury Jr P. T. (1993) The carboxy terminus of the beta amyloid protein is critical for the seeding of amyloid formation: implications for the pathogenesis of Alzheimer's disease. *Biochemistry* **32**, 4693–4697.

Kayed R., Head E., Thompson J. L., McIntire T. M., Milton S. C., Cotman C. W. and Glabe C. G. (2003) Common structure of soluble amyloid oligomers implies common mechanism of pathogenesis. *Science* **300**, 486–489.

Klafki H. W., Wiltfang J. and Staufenbiel M. (1996) Electrophoretic separation of betaA4 peptides (1-40) and (1-42). *Anal. Biochem.* **237**, 24–29.

Lambert M. P., Barlow A. K., Chromy B. A. *et al.* (1998) Diffusible, nonfibrillar ligands derived from Abeta1-42 are potent central nervous system neurotoxins. *Proc. Natl Acad. Sci. USA* **95**, 6448–6453.

Lemere C. A., Blusztajn J. K., Yamaguchi H., Wisniewski T., Saido T. C. and Selkoe D. J. (1996) Sequence of deposition of heterogeneous amyloid beta-peptides and APO E in Down syndrome: implications for initial events in amyloid plaque formation. *Neurobiol. Dis.* **3**, 16–32.

Lesne S., Koh M. T., Kotilinek L., Kayed R., Glabe C. G., Yang A., Gallagher M. and Ashe K. H. (2006) A specific amyloid-beta protein assembly in the brain impairs memory. *Nature* **440**, 352–357.

Miravalle L., Calero M., Takao M., Roher A. E., Ghetti B. and Vidal R. (2005) Amino-terminally truncated Abeta peptide species are the main component of cotton wool plaques. *Biochemistry* **44**, 10810–10821.

Murakami K., Irie K., Morimoto A., Ohigashi H., Shindo M., Nagao M., Shimizu T. and Shirasawa T. (2003) Neurotoxicity and physicochemical properties of Abeta mutant peptides from cerebral amyloid angiopathy: implication for the pathogenesis of cerebral amyloid angiopathy and Alzheimer's disease. *J. Biol. Chem.* **278**, 46179–46187.

Nimmrich V., Grimm C., Draguhn A., Barghorn S., Lehmann A., Schoemaker H., Hillen H., Gross G., Ebert U. and Bruehl C. (2008) Amyloid beta oligomers (A beta(1-42) globulomer) suppress spontaneous synaptic activity by inhibition of P/Q-type calcium currents. *J. Neurosci.* **28**, 788–797.

Piccini A., Russo C., Gliozzi A. *et al.* (2005) {beta}-amyloid is different in normal aging and in Alzheimer disease. *J. Biol. Chem.* **280**, 34186–34192.

Rönicke R., Schroder U. H., Bohm K. and Reymann K. G. (2009) The Na+/H+ exchanger modulates long-term potentiation in rat hippocampal slices. *Naunyn. Schmiedebergs. Arch. Pharmacol.* **379**, 233–239.

Rönicke R., Mikhaylova M., Ronicke S., Meinhardt J., Schroder U. H., Fandrich M., Reiser G., Kreutz M. R. and Reymann K. G. (2011) Early neuronal dysfunction by amyloid beta oligomers depends on activation of NR2B-containing NMDA receptors. *Neurobiol. Aging* **32**, 2219–2228.

Russo C., Schettini G., Saido T. C., Hulette C., Lippa C., Lannfelt L., Ghetti B., Gambetti P., Tabaton M. and Teller J. K. (2000) Presenilin-1 mutations in Alzheimer's disease. *Nature* **405**, 531–532.

Schilling S., Lauber T., Schaupp M., Manhart S., Scheel E., Bohm G. and Demuth H. U. (2006) On the seeding and oligomerization of pGlu-amyloid peptides (in vitro). *Biochemistry* **45**, 12393–12399.

Schilling S., Zeitschel U., Hoffmann T. *et al.* (2008) Glutaminyl cyclase inhibition attenuates pyroglutamate Abeta and Alzheimer's disease-like pathology. *Nat. Med.* **14**, 1106–1111.

Schlenzig D., Manhart S., Cinar Y., Kleinschmidt M., Hause G., Willbold D., Funke S. A., Schilling S. and Demuth H. U. (2009) Pyroglutamate formation influences solubility and amyloidogenicity of amyloid peptides. *Biochemistry* **48**, 7072–7078.

Shankar G. M., Li S., Mehta T. H. *et al.* (2008) Amyloid-beta protein dimers isolated directly from Alzheimer's brains impair synaptic plasticity and memory. *Nat. Med.* **14**, 837–842.

Shirotani K., Tsubuki S., Lee H. J., Maruyama K. and Saido T. C. (2002) Generation of amyloid beta peptide with pyroglutamate at position 3 in primary cortical neurons. *Neurosci. Lett.* **327**, 25–28.

Townsend M., Shankar G. M., Mehta T., Walsh D. M. and Selkoe D. J. (2006) Effects of secreted oligomers of amyloid beta-protein on hippocampal synaptic plasticity: a potent role for trimers. *J. Physiol.* **572**, 477–492.

Walsh D. M. and Selkoe D. J. (2004) Deciphering the molecular basis of memory failure in Alzheimer's disease. *Neuron* **44**, 181–193.

Walsh D. M., Hartley D. M., Condron M. M., Selkoe D. J. and Teplow D. B. (2001) In vitro studies of amyloid beta-protein fibril assembly and toxicity provide clues to the aetiology of Flemish variant (Ala692–>Gly) Alzheimer's disease. *Biochem. J.* **355**, 869–877.

Walsh D. M., Townsend M., Podlisny M. B., Shankar G. M., Fadeeva J. V., Agnaf O. E., Hartley D. M. and Selkoe D. J. (2005) Certain inhibitors of synthetic amyloid beta-peptide (Abeta) fibrillogenesis block oligomerization of natural Abeta and thereby rescue long-term potentiation. *J. Neurosci.* **25**, 2455–2462.